Compact Antenna for Microsatellite Using Folded Shorted Patches and an Integrated Feeding Network

S.K. Podilchak[1], M. Caillet[1], D. Lee[1], Y.M.M. Antar[1],
L. Chu[2], J. Cain[2], M. Hammar[2], D. Caldwell[2], E. Barron[2]

[1]Department of Electrical and Computer Engineering, Royal Military College of Canada
13 General Crerar Crescent, Kingston, Ontario, Canada, K7K 7B4

[2]COM DEV International Inc., 60 Struck Court, Cambridge, Ontario, Canada, N1R 8L2

***Abstract*— This article focuses on the design and operation of a circularly polarized (CP) antenna unit for space applications using a four element array of folded-shorted patches. The metallic antenna structure is low-profile, ultra-compact ($0.2\lambda_0$ by $0.2\lambda_0$), and offers good CP performance at 400 MHz. Specifically, the four probe fed patch elements are placed in a sequential rotation configuration, while a miniaturized hybrid coupler based feeding network provides a 90° phase difference between the radiating elements. The feeding circuit is integrated on the underside of the antenna ground plane and a back plate housing encloses the printed circuit board. Measurements and simulations are in good agreement and the compact antenna unit may be useful for space communication systems using microsatellites and miniaturized phased arrays for security, surveillance, and other beam steering and direction finding applications.**

I. Introduction

Small satellites, or microsatellites, are transforming space-based surveillance systems [1]. Typical configurations include a network of small satellites that can offer increased coverage and enhanced data collection rates when compared to conventional large scale systems. Applications include marine vehicle tracking, crop growth analysis, ice flow monitoring, and climate change observation. Microsatellites can also reduce launching costs and mission development time, thus making remote sensing technologies more cost effective.

In this work we propose a highly compact and low profile circularly polarized (CP) antenna for 400 MHz microsatellite applications. Specifically a new antenna structure is presented using a four element array of folded-shorted multilayer patches [2]-[5] as shown in Figs. 1 and 2. To ensure a reduced foot print for the antenna unit, the individual elements were closely spaced on a $0.2\lambda_0$ by $0.2\lambda_0$ ground plane platform. In addition, an ultra-compact feeding network (Fig. 3) was integrated into the bottom side of the antenna ground plane to achieve quadrature excitation [6]-[9] of the individual folded-shorted patch elements for right-handed circular polarization (RHCP). A simulation model (Fig. 4) was also developed to ensure antenna performance was optimized, as well as the relative element positioning, for 400 MHz operation.

To the author's knowledge this is the first time that such a miniaturized and low-profile CP antenna unit has been presented using an integrated feeding network printed circuit board (PCB). In addition, the compact antenna design is not limited to UHF satellite communications but may also

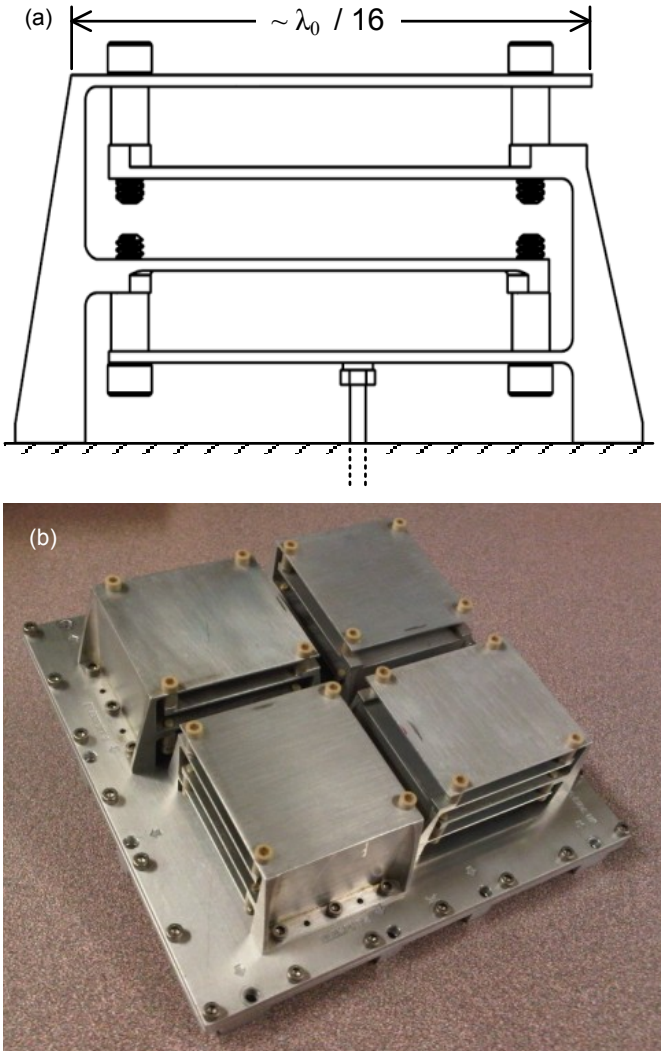

Fig. 1. (a): Single radiating patch element realized by four metallic layers, two support brackets, and a probe feed. (b): An arrayed configuration of four elements defines the complete antenna structure. A compact feeding network was bonded to the underside of the $0.2\lambda_0$ by $0.2\lambda_0$ ground plane platform.

be useful for military and radar applications, compact array designs with integrated feeding networks for beam steering, and other phased array systems. Moreover, this configuration of folded-shorted antenna patches is not restricted to metallic topologies but could also be implemented in a dielectric multilayer technology for large scale integration with other

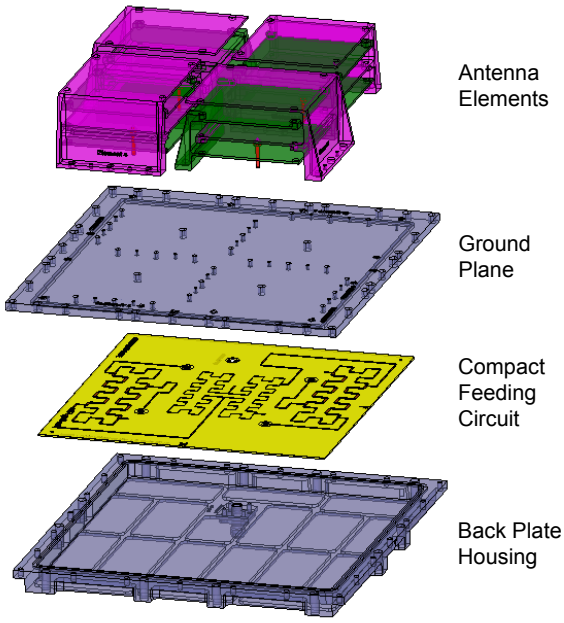

Fig. 2. Illustrated stackup of the complete antenna structure: four elements, ground plane platform, feeding network PCB, and back plate housing.

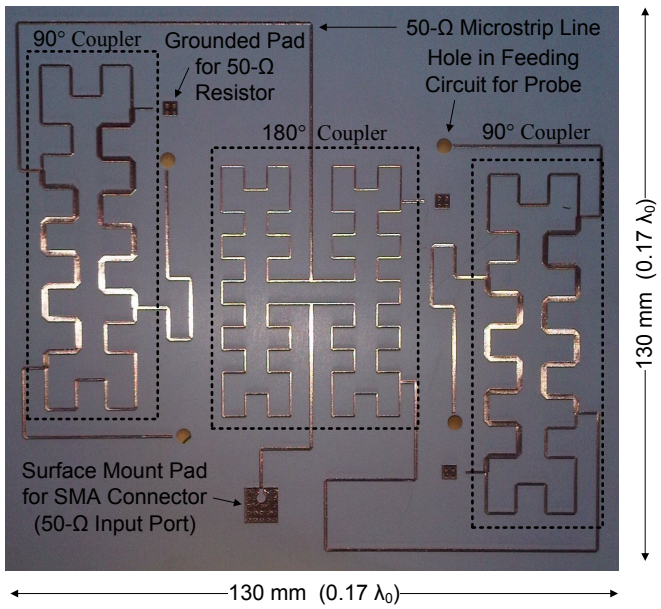

Fig. 3. Compact feeding circuit bonded to the bottom side of the ground plane. A network of three couplers (using meandered transmission lines) was designed to achieve quadrature excitation for CP operation. Substrate holes were also included for probe connectivity to the top radiating elements and a SMA connector defines the single input port for the complete antenna unit.

circuit and antenna devices. For instance, by scaling the appropriate dimensions of the folded patch elements (layer size, vein separation, and probe position), antenna performance can be optimized and adjusted for the required frequency of operation.

II. Antenna Design Considerations

Miniaturization of the conventional half-wave patch antenna is a topic of considerable interest within the electromagnetics community. Techniques to reduce the physical size of printed designs include the use of high dielectric constant materials [10]. But narrowed bandwidth performance can be observed with these designs along with reduced radiation efficiencies. Other strategies for size reduction include additional shorting pins near the probe feed, shape optimization, and spur-line notching [11]-[14]. These design challenges may be avoided by the choice of low dielectric constant materials and the inclusion of a metallic shorting wall [2] where patch radiating lengths can be reduced to approximately 25% of the guided wavelength. Using this design, multilayer configurations have been further developed by the intricate inward folding of the shorted patch and ground plane [3]-[5]. This reduction methodology is made possible by image theory [14]. Four and six layered structures have also been developed [4] with respective antenna radiating lengths of only 6.3% and 4.2% of the free space wavelength.

A. Design Procedure, Antenna Assembly, & Simulation

The four folded-shorted patch elements were individually machined, assembled, and placed on top of an intermediate ground plane platform (Fig. 5). The metallic folded antenna layers were separated and secured by PEEK (Polyether ether ketone) spacers and screws. The side brackets of the metallic elements were secured to the ground plane using steel fasteners. Four probes, inserted through the ground plane, excite the individual antenna elements. The compact feeding network using meandered transmission lines and hybrid couplers (Fig. 3) was bonded to the underside of the ground plane to excite the individual elements in quadrature [7]. The utilized meander technique is based on a modified space-filling curve [15], and for both hybrid couplers, a portion of Moore's 2nd iteration curve was used to implement the circuit topologies. A back plate housing encapsulates the feeding circuit and a SMA connector jack defines the single input port of the antenna.

Optimization techniques in HFSS [16] were initially employed to achieve good reflection losses and CP radiation performance. The antenna simulation model is shown in Fig. 4 and results are compared to measurements in Figs. 8 and 9 and Tables I - III. Essentially the folded-shorted patch sizes, element spacing, vein separation, and probe positions were first optimized to achieve good reflection losses and CP performance values at 400 MHz; ie. $|S_{11}| \leq -20$ dB and antenna gain ≥ 2.5 dBic at boresight. Based on these optimized dimensions antenna parts were machined from solid aluminum, assembled on the intermediate ground plane (Fig. 5), and then tested to ensure functionality.

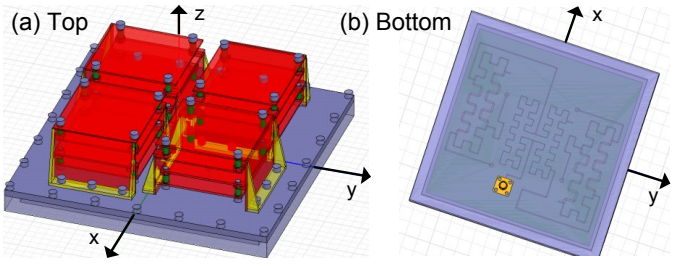

Fig. 4. Simulation model with back plate enclosure and feeding circuit PCB.

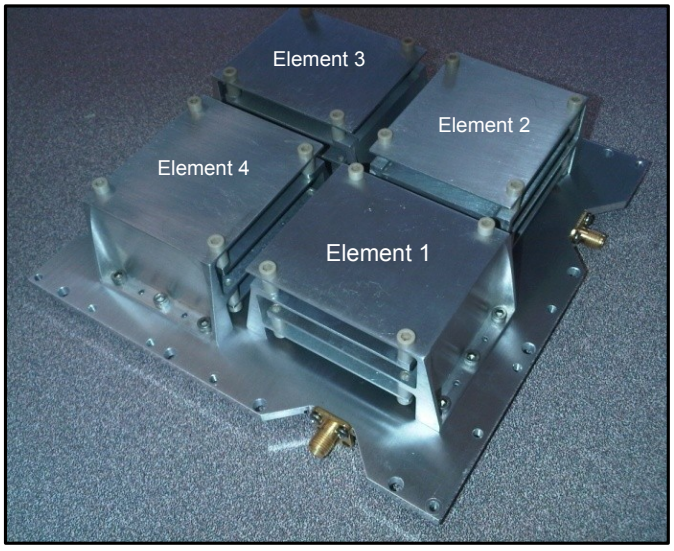

(a) Intermediate Testing Structure

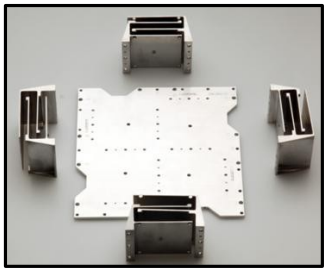

(b) Element Assembly

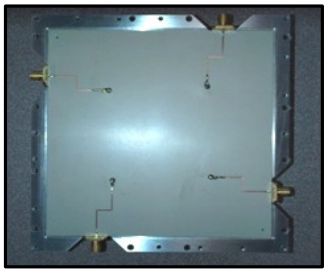

(c) Bottom Side Feed

Fig. 5. Radiating elements were placed on an intermediate ground plane to individually test functionality. A simplified PCB feed was employed (probe connection via microstrip lines and four SMA connectors) with no back plate enclosure. During measurement trials quadrature excitation was achieved by using calibrated cables and modular component couplers to realize RHCP.

B. Dual-Orthogonal Mode Excitation

Circular polarization can be achieved with patches using two methods: by simultaneously exiting two orthogonal degenerate modes, or by using a dual-orthogonal feed [6]-[9], [14]. It has been established that circular polarization can be generated using linearly polarized elements [6], and by using four elements in a square configuration it is possible to obtain low cross-polarization levels over a wider beamwidth and frequency bandwidth [7], [8] and thus such a topology was utilized in the antenna design. In addition, it is challenging to excite two degenerate modes with the folded-shorted patches due to the shorting walls. Patch notching or the inclusion of spur-lines could also have been used in the element designs for circular polarization but would have been difficult to implement within the four layers. For these reasons, a four element array of folded-short patches using a feeding network was used to generate RHCP.

C. Integrated Feeding Network Using Meandered Microstrip Lines and Hybrid Couplers

An ultra-compact feeding circuit was required as the entire antenna structure ($0.2\lambda_0$ by $0.2\lambda_0$) was smaller than the communications wavelength. More specifically, the feeding circuit employed one 180° hybrid and two 90° hybrid couplers

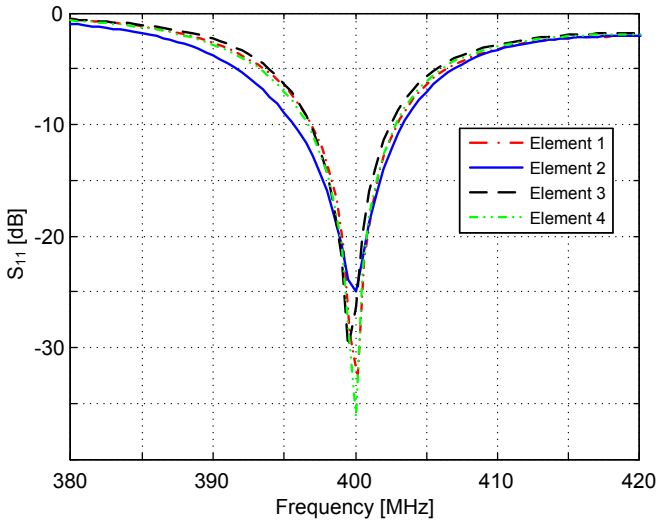

Fig. 6. Measured $|S_{11}|$ of the individual folded patch elements (Fig. 5(a)).

to achieve the required phase quadrature between each antenna element for RHCP (a reverse sequential phase feeding could also lead to the opposite polarization). In addition, the 50-Ω input SMA connector provides connectivity to the coaxial probes (which excites the antenna elements) via a network of meandered transmission lines as shown in Fig. 3.

The challenge with implementing a feeding network for such an ultra-compact antenna design is the small 130 mm by 130 mm footprint available ($0.17\lambda_0$ by $0.17\lambda_0$). This footprint is dictated by the finite $0.2\lambda_0$ by $0.2\lambda_0$ ground plane platform and the mechanical fasteners required for encapsulation as well as stabilizing the assembled antenna unit to the microsatellite structure. As such the feeding circuit PCB could not extent to the edge of the ground plane platform. Furthermore, the back plate enclosure should not affect the feeding circuit performance or significantly vary the resonant frequencies of

TABLE I
SINGLE ELEMENT INPUT MATCH
(INTERMEDIATE TESTING STRUCTURE)

	Frequency for Minimum Reflection Coefficient [MHz]	Corresponding VSWR (50Ω Impedance)
Simulation :		
Element 1	400	1.07:1
Element 2	400	1.07:1
Element 3	400	1.07:1
Element 4	400	1.07:1
Measurement :		
Element 1	398.5	1.05:1
Element 2	400.0	1.12:1
Element 3	399.5	1.07:1
Element 4	400.0	1.03:1

Note: The folded-shorted patch elements were measured and compared to simulations to ensure individual functionality. The intermediate ground plane platform (antenna testing structure of Fig. 5(a)) was utilized during testing. Measurement values are also plotted as a function of frequency in Fig. 6.

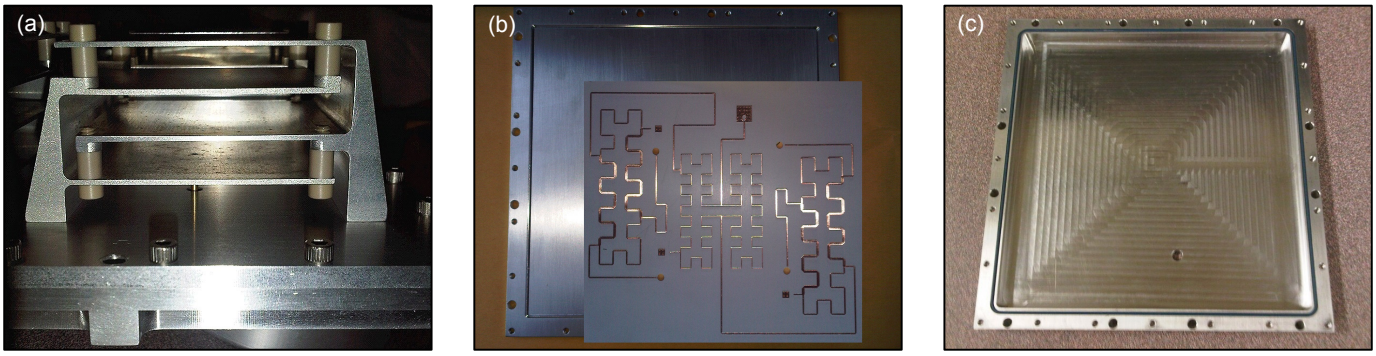

Fig. 7. The radiating elements were assembled and then placed on the final ground plane (with the integrated feeding network bonded to the underside of the platform) with a back plate enclosing the feeding circuit. A single SMA connector defines the input port for the assembled antenna (shown in Fig. 1(b)).

the antenna elements on the top side of the ground plane. To ensure fields were fairly bound to the substrate a high dielectric constant material with low loss ($\epsilon_r = 10.2, \tan\delta = 0.0023$) was chosen to implement the PCB design.

III. Results & Discussion

The antenna structure was simulated using HFSS [16]. Results are compared to the measurements in Figs. 6, 8 - 11 and Tables I - III. Measured gain values are greater than 2 dBic at boresight from 393.5 MHz to 401.5 MHz for both the intermediate testing structure (Fig. 5(a)) and the fully assembled antenna unit (Fig. 1(b)). In addition, results are in good agreement with the simulated beam patterns and the presented antenna configurations also provide low cross-polarization levels in the boresight direction; ie. left-handed circular polarized (LHCP) levels (cross-polarization) are less than 10 dB from the RHCP boresight maximum from 396 to 404 MHz. Measured axial ratios are less than 3 dB from -40° to + 40° as also shown in Fig. 10.

TABLE II
Radiation Characteristics
(Intermediate Testing Structure)

	Simulation		Measurement		
Frequency [MHz]	398	402	397	399	401
RHCP Gain [dBic] :					
$\theta = 0°$	+2.6	+1.5	+2.1	+2.3	+2.2
$\theta = \pm 65°$	-1.0	-2.1	-1.5	-1.3	-1.4
X-Pol. Level [dB] :					
$\theta = 0°$	< 40	< 40	< 15	< 17	< 19
$\theta = \pm 65°$ (below RHCP Maximum)	< 14	< 14	< 6	< 7	< 12
Axial Ratio [dB] :					
$-40° < \theta < +40°$	< 3	< 3	< 3	< 3	< 3

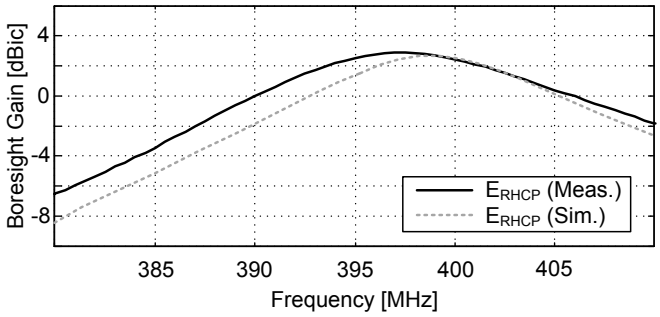

Fig. 8. Realized boresight gain for the antenna testing structure (Fig. 5(a)).

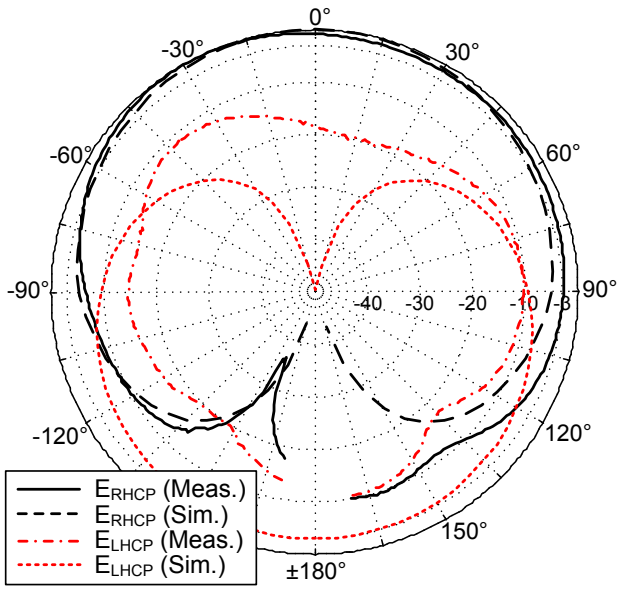

Fig. 9. Normalized beam patterns at 400 MHz for the intermediate antenna testing structure (Fig. 5(a)). Results are shown in the x-z plane ($\phi = 0°$).

The downward frequency shift between the measurements and the simulations may be attributed to fabrication tolerances, minor probe misalignment, and the possible interference of the measurement cables attached to the SMA connector. In addition, minor details within the developed HFSS simulation model (Fig. 4) were excluded for reduced computations and moderate simulation time, but it should be stressed that

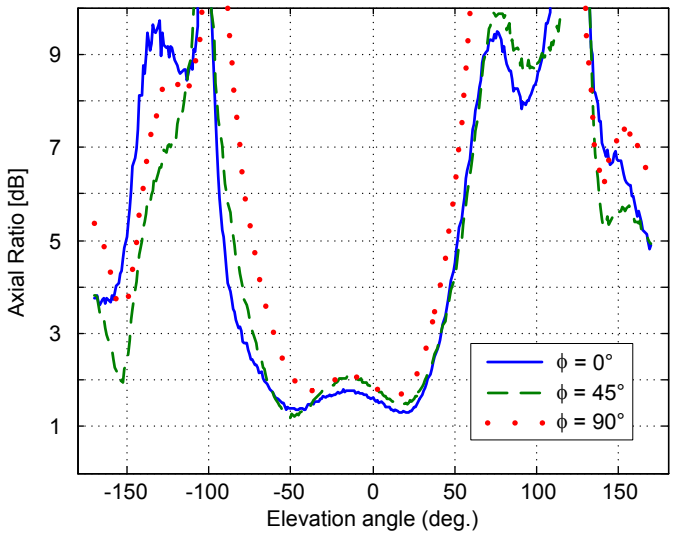

Fig. 10. Measured axial ratio at 399 MHz for the intermediate antenna testing structure (Fig. 5(a)). Axial ratios are less than 3 dB from -58° to +42°

the major dimensions of the studied antenna (folded-shorted patch elements, metallic support brackets, ground plane, back plate housing, feeding circuit, probes, and SMA jack) were fully described. For example, the diameter and length of the stainless steel fasteners was incorporated into the simulation model but the threading depth was not. These minor details were excluded for all antenna elements and may also contribute to the observed discrepancies. In effect, a simplified simulation model was developed, but despite these modeling challenges and fabrication practicalities, measurement results are in agreement with the simulations and a good proof of concept for the antenna structure is observed.

IV. Conclusion

This paper investigates an ultra-compact antenna structure using a four element arrayed configuration of folded-shorted patches for operation at 400 MHz. Right-handed circular polarization is achieved by the addition of a compact feeding circuit integrated into the ground plane of the antenna structure for quadrature excitation. Initially design concepts are discussed followed by an analysis of the antenna performance. Measurements are also provided for the compact antenna unit and experimental values are in close agreement with the simulations.

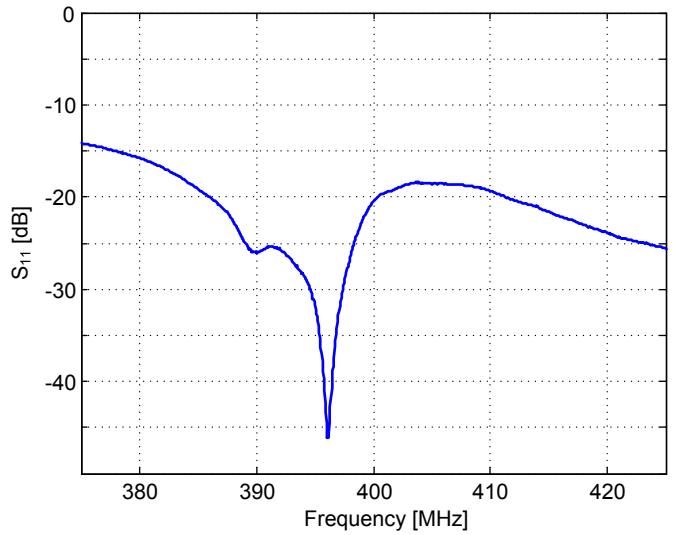

Fig. 11. Measured $|S_{11}|$ for the fully assembled antenna structure (Fig. 1).

TABLE III
Fully Assembled Antenna Input Match

	Simulation	Measurement
Frequency Bandwidth [MHz]	395 ± 10	393.5 ± 7
VSWR (50Ω Impedance)	1.20:1	1.20:1

Note: Results shown here for the full antenna structure (Fig. 1).

References

[1] S. Gao, K. Clark, A. Sharaiha, M. Unwin, J. Zackrisson, W.A. Shiroma, J.M. Akagi, K. Maynard, P. Garner, L. Boccia, G. Amendola, G. Massa, C. Underwood, M. Brenchley, M. Pointer, and M.N. Sweeting, "Antennas for Modern Small Satellites," *IEEE Antennas and Propagation Magazine*, vol. 51, no. 4, pp. 40-56, Aug. 2009.

[2] S. Pinhas and S. Shtrikman, "Comparison Between Computed and Measured Bandwidth of Quarter-Wave Microstrip Radiators," *IEEE Trans. Ant. Prop.*, vol. 36, no. 11, pp. 1615-1616, Nov. 1988.

[3] R. Li, G. DeJean, M. M. Tentzeris, and J. Laskar, "Development and Analysis of a Folded Shorted-Patch Antenna With Reduced Size," *IEEE Trans. Ant. Prop.*, vol. 52, no. 2, pp. 555–562, Feb. 2004.

[4] J. Zhang and O. Breinbjerg, "Miniaturization of Multiple-Layer Folded Patch Antennas," *European Conference on Antennas and Propagation*, pp. 3502–3506, 23-27 Mar. 2009.

[5] A. Holub and M. Polivka, "Vertically Meander-Folded, Shorted-Patch Antennas," *Wiley Microwave and Optical Tech. Lett.*, vol. 51, no. 12, pp. 2938–2942, Dec. 2009.

[6] J. Huang,"A Technique for an Array to Generate Circular Polarization with Linearly Polarized Elements," *IEEE Trans. Ant. Prop.*, vol. 34, no. 9, pp. 1113-1124, Sep. 1986.

[7] R. Bauer and J. Schuss, "Axial ratio of balanced and unbalanced fed circularly polarized patch radiator arrays," *IEEE AP-S Int. Symp.*, vol. 25, pp. 286-2-89, Jun. 1987.

[8] M. Caillet, M. Clénet, A. Sharaiha, and Y.M.M Antar, "A Compact Wide-Band Rat-Race Hybrid using Microstrip Lines," *IEEE Microw. Wireless Compon. Lett.*, vol. 19, no. 4, pp. 191-193, Apr. 2009.

[9] M. Caillet, M. Clénet, A. Sharaiha, and Y.M.M Antar, "A Broadband Folded Printed Quadrifilar Helical Antenna Employing a Novel Compact Planar Feeding Circuit," *IEEE Trans. Ant. Prop.*, vol. 58, no. 7, pp. 2203-2209, Jul. 2010.

[10] T. K. Lo, C.-O. Ho, Y. Hwang, E. K. W. Lam, and B. Lee, "Miniature Aperture-Coupled Microstrip Antenna of Very High Permittivity," *IET Electronics Letters*, vol. 33, no. 1, pp. 9-10, Jan. 1997.

[11] R. B. Waterhouse, S. D. Targonski, and D. M. Kokotoff, "Design and Performance of Small Printed Antennas," *IEEE Trans. Ant. Prop.*, vol. 46, no. 11, pp. 1629-1633, Nov. 1998.

[12] K.L. Wong and K.P. Yang, "Modified planar inverted F antenna," *IET Electronics Letters*, vol. 34, no. 1, pp. 7-8, Jan. 1998.

[13] W.S. Chen, K.L. Wong, and C.K. Wu, "Inset microstripline-fed circularly polarized microstrip antennas," *IEEE Trans. Ant. Prop.*, vol. 48, no. 8, pp. 1253-1254, Aug. 2004.

[14] R. Garg et al., "Microstrip antenna design handbook," Artech House Publishers, Norwood, MA, USA 2001.

[15] H. Sagan, "Space-Filling Curves," Springer-Verlag, 1994.

[16] "High Frequency Structure Simulator v. 11.0," Ansoft Corp, 2012 [Online]. Available: www.ansys.com